

# Molecular orientation induced by $H^+$ collision and modulated with combined fields

Zhiwei Ge (葛志伟)<sup>1</sup>, Xuequn Hou (侯学群)<sup>2</sup>, Yu Zhao (赵宇)<sup>1</sup>, and Qingtian Meng (孟庆田)<sup>1\*</sup>

<sup>1</sup>School of Physics and Electronics, Shandong Normal University, Jinan 250358, China

<sup>2</sup>Shandong Labor Vocational and Technical College, Jinan 250022, China

\*Corresponding author: [qtmeng@sdu.edu.cn](mailto:qtmeng@sdu.edu.cn)

Received June 15, 2021 | Accepted September 6, 2021 | Posted Online October 15, 2021

We take  $H^+ + CO$  as a prototype to analyze the effect of ion or proton collision on molecular orientation modulated by a two-color shaped pulse combined with the time-delayed terahertz (THz) pulse. Through examining the effect of ion collision on the molecular orientation, we found that when the impact parameter and collisional velocity have weak inverse influences on the maximal orientation degree, the appropriate two-color and THz field intensity employed can improve the molecular orientation degree. The carrier envelope phase and frequency of the THz laser pulse as well as the temperature also have certain influence on the collision-induced molecular orientation.

**Keywords:** ion collision; orientation; combined fields.

**DOI:** [10.3788/COL202119.110201](https://doi.org/10.3788/COL202119.110201)

## 1. Introduction

The alignment and orientation of molecules have important and comprehensive application value in photoelectron angular distribution, chemical reaction dynamics, high-order harmonic generation, photoionization, photodissociation, and so on<sup>[1–13]</sup>. Alignment denotes that the molecular axis is parallel or perpendicular to the polarization direction of the laser, whereas the orientation requires not only a fixed direction but also a particular order of head versus tail. Therefore, the orientation of molecules has a larger difficulty than the alignment. With the progress of laser technology, the collision-induced alignment and orientation under external fields have aroused the attention of many physicists and chemists. The collision processes take place between ion and atom or molecule<sup>[14,15]</sup>, atom and atom<sup>[16,17]</sup>, as well as atom and molecule<sup>[18,19]</sup>. Being acquainted with these collision processes is beneficial not only to manipulate the molecular orientation and laser-induced chemistry, but also to understand the related molecular dynamics in depth.

The ion-impact excitation of the diatomic molecule has been widely investigated in the absence of the laser field<sup>[20]</sup> both experimentally and theoretically. With the advancement of laser technology, various shape pulses, pulse chains, and combinations of different pulses have appeared and been used to explore the energy transfer processes and molecular orientation in collisions, among which the laser-assisted ion–molecule collision is one of the hottest research topics. In 1991, Mohan *et al.*<sup>[21]</sup> used the non-perturbed Floquet theory to depict the ion and molecule

collisions and developed the vibrational excitation theory of diatomic molecules due to the collision between the ion ( $He^+$ ) and carbon monoxide (CO) molecule under an infrared laser beam. Madsen *et al.*<sup>[14]</sup> explored the excitation mechanisms in vigorous ion–atom collisions inside sub-femtosecond laser pulses and obtained that single electron dynamics in two external fields may result in new coherence effects. When an ion or proton collides with a diatomic molecule, besides the collision energy and the original state of collision partners, the relative orientation of the target molecule is also a significant element to determine this collision consequence. Van Beek *et al.*<sup>[22]</sup> investigated the influence of molecular orientation on rotationally inelastic collision of  $OH(X^2\Pi)$  with Ar exposed to the narrow band dye laser and found that the probability density function of orientation was confirmed by laser-induced fluorescence spectroscopy. Brouard *et al.*<sup>[23]</sup> explored the rotational angular momentum orientation influences on the inelastic collision of NO with Ar by employing a hexapole electric field and discussed the origin of collision-induced orientation using quantum mechanical hard shell, classical hard shell, and quasi-classical trajectories calculation methods. Some researches showed that in the dissociation of molecular ions, such as  $GaN^{2+}$  and  $AlN^{2+}$ <sup>[24]</sup> as well as phosphorus molecular ions<sup>[25]</sup> during laser-assisted atomic probe tomography, different orientations of molecular ions could give rise to different dissociation yields. So, we can find that the molecular orientation plays significant roles in the investigation of not only molecular collisions, but also photodissociation dynamics aspects.

When exploring the molecular orientation, one often takes into account the influence of the external field. In the early days, the strong electrostatic field was usually used to control polar molecule orientation. The relevant experimental research showed that the hexapole electric field has advantages in orienting polarity symmetrical top or symmetrical top-like molecules<sup>[26]</sup>. Because of the not high degree of single field-induced molecular orientation degree, it is found that the combined fields can be a choice to improve the molecular orientation. Friedrich *et al.*<sup>[27]</sup> enhanced the orientation degree of polar molecules by combining the static field and the intense non-resonant laser pulse. Cai *et al.*<sup>[28]</sup> studied the time evolution of the state created by non-adiabatic interaction of a polar molecule with the combination of electrostatic and pulsed non-resonant laser fields. Later, the two-color laser pulse<sup>[29,30]</sup> and the multi-color laser pulse<sup>[31]</sup> are applied to improve the molecular orientation through the interaction with molecular hyperpolarizability. Due to the low energy of the terahertz (THz) laser pulse causing less damage to molecules, and, what is more, as the frequency of transition between rotation energy levels of molecules is usually at the THz scale, various THz laser pulses and shaped laser pulses were used to explore the molecular alignment and orientation, such as the THz laser pulse of half-cycle<sup>[32,33]</sup>, slow turn-on and rapid turn-off (STRT) laser pulse<sup>[34]</sup>, as well as elliptically polarized laser pulse<sup>[35]</sup>. Then, the non-resonant laser pulse combined with the THz laser pulse is extensively used for molecular orientation<sup>[36,37]</sup>. Although many works about the effect of collision in various external fields have been done, there are few detailed reports on the combined external field modulation of the collision-induced orientation. In this Letter, we present the investigation of using the combined field by a two-color field and time-delayed THz laser pulse to modulate the  $H^+ + CO$  collision-induced molecular orientation.

The following explains how this Letter is arranged. Section 2 mainly outlines the density matrix theory method used in the calculation. In Section 3, we give the time evolution of the orientation degree in absence of an external field and how it is steered by laser pulses, and the influences of interaction potential and laser pulse parameters on molecular orientation degree are discussed and analyzed. Meanwhile, the influence of different temperatures on orientation is also compared. Finally, conclusions and perspectives are given in Section 4.

## 2. Theoretical Method

The molecular orientation was studied by considering the collision between an ion A and a diatomic molecule BC under a two-color laser pulse with STRT and a time-delayed THz laser pulse. The two-color laser pulse is expressed as

$$E_{\text{STRT}}(t) = E_1(t)[\cos \omega_1 t + (\cos 2\omega_1 t)], \quad (1)$$

with

$$E_1(t) = E_{01} \exp(-t^2/2\sigma^2), \quad (2)$$

where  $E_{01}$  represents the electric field amplitude,  $\omega_1$  and  $2\omega_1$  are the fundamental frequency and the second harmonic frequency,

respectively,  $\sigma = \sigma_r$  ( $t \leq 0$ ) and  $\sigma = \sigma_f$  ( $t \geq 0$ ) are the rising and falling times of the two-color laser pulse with  $\sigma_r \gg \sigma_f$ . The THz laser pulse can be written as

$$E_{\text{THz}}(t) = E_2(t) \cos[\omega_{\text{THz}}(t - t_d + \varphi)], \quad (3)$$

with

$$E_2(t) = E_{02} \exp[-2 \ln 2(t - t_d)^2/\tau^2], \quad (4)$$

where  $E_{02}$ ,  $\omega_{\text{THz}}$ ,  $\tau$ ,  $t_d$ , and  $\varphi$  denote the intensity of the THz field, frequency, full width at half-maximum (FWHM), delay time between two-color and THz laser pulses, and carrier envelope phase (CEP), respectively.

The interaction potential between the ion or proton A and molecule BC is described by<sup>[21]</sup>

$$V_c(r, R, \gamma) = -\frac{\mu(r) \cdot R}{R^3} = -\frac{\mu(r)}{R^2} \cos \gamma, \quad (5)$$

where  $R$  is the distance between the ion or proton A and center of mass of the molecule BC,  $r$  is the internuclear distance between B and C,  $\gamma$  is the angle between  $R$  and  $r$  (Fig. 1), and  $\mu(r)$  is the dipole moment operator of the molecule. Meanwhile,

$$\cos \gamma = \frac{vt}{R} \cos \theta - (1 - \cos^2 \theta)^{\frac{1}{2}} \cdot \frac{b}{R}, \quad (6)$$

$$R(t) = b + vt, \quad (7)$$

where  $v$  denotes the relative collision velocity between the ion and the diatomic molecule,  $b$  is the impact parameter, and  $\theta$  is the angle between the polarization vector of the laser pulse and the rotational angular momentum of the BC. According to the Taylor formula,  $(1 - \cos^2 \theta)^{\frac{1}{2}}$  can be approximately written as  $1 - \frac{1}{2} \cos^2 \theta$  since, generally,  $\cos \theta < 1$ . Under the rigid rotor approximation, the total Hamiltonian of this system can be expressed as

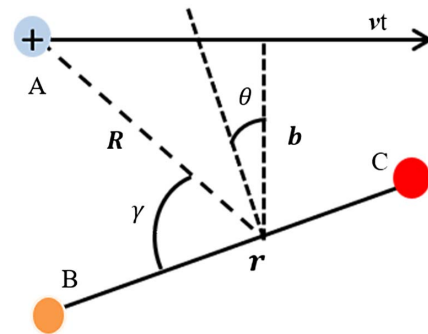


Fig. 1. Schematic diagram of the coordinate system formed by the collision of an ion or proton with a molecule.

$$\begin{aligned} \hat{H}(t) = & B_e \hat{J}^2 - \mu E_{\text{THz}}(t) \cos \theta - \frac{1}{4} [(\alpha_{\parallel} - \alpha_{\perp}) \cos^2 \theta \\ & + \alpha_{\perp}] E_1^2(t) - \frac{1}{8} [(\beta_{\parallel} - 3\beta_{\perp}) \cos^3 \theta + 3\beta_{\perp} \cos \theta] E_1^3(t) \\ & + V_c(r, R, \gamma), \end{aligned} \quad (8)$$

where  $B_e$  is the rotational constant of the molecule BC,  $\hat{J}$  is the angular momentum operator, and  $\alpha_{\parallel}$  ( $\beta_{\parallel}$ ) and  $\alpha_{\perp}$  ( $\beta_{\perp}$ ) are the polarizability (hyperpolarizability) parallel and perpendicular to the molecular axis, respectively. The molecule orientation degree is expressed as

$$\langle \cos \theta \rangle = \text{Tr}\{\cos \theta \hat{\rho}(t)\}, \quad (9)$$

where Tr represents the trace of the matrix, and  $\hat{\rho}(t)$  is the time-dependent density operator. Using the Liouville equation, the time evolution of the density operator is given as

$$\frac{d\hat{\rho}(t)}{dt} = -\frac{i}{\hbar} [\hat{H}, \hat{\rho}(t)]. \quad (10)$$

In the eigenstates of the rigid rotor Hamiltonian, the density operator is written as

$$\hat{\rho}(t) = \sum_{J, M, J', M'} \rho_{JM|J'M'}(t) |JM\rangle \langle J'M'|, \quad (11)$$

where  $\rho_{JM|J'M'}(t)$  are decided by coupling differential equations,

$$\begin{aligned} \frac{d\rho_{JM|J'M'}(t)}{dt} = & -\frac{i}{\hbar} \{(\epsilon_J - \epsilon_{J'}) \rho_{JM|J'M'} \\ & - \frac{\mu \nu t}{(b^2 + \nu^2 t^2)^{\frac{3}{2}}} \sum_{J_1 M_1} [V_{JM|J_1 M_1}^{(1)} \rho_{J_1 M_1 | J' M'}(t) \\ & - V_{J_1 M_1 | J' M'}^{(1)} \rho_{JM|J_1 M_1}(t)] \\ & - \frac{\mu b}{2(b^2 + \nu^2 t^2)^{\frac{3}{2}}} \sum_{J_1 M_1} [V_{JM|J_1 M_1}^{(2)} \rho_{J_1 M_1 | J' M'}(t) \\ & - V_{J_1 M_1 | J' M'}^{(2)} \rho_{JM|J_1 M_1}(t)] \\ & - \mu E_{\text{THz}}(t) \sum_{J_1 M_1} [V_{JM|J_1 M_1}^{(1)} \rho_{J_1 M_1 | J' M'}(t) \\ & - V_{J_1 M_1 | J' M'}^{(1)} \rho_{JM|J_1 M_1}(t)] \\ & - \frac{1}{4} \Delta \alpha E^2(t) \sum_{J_1 M_1} [V_{JM|J_1 M_1}^{(2)} \rho_{J_1 M_1 | J' M'}(t) \\ & - V_{J_1 M_1 | J' M'}^{(2)} \rho_{JM|J_1 M_1}(t)] - \frac{1}{8} E^3(t) \sum_{J_1 M_1} \{(\beta_{\parallel} \\ & - 3\beta_{\perp}) V_{JM|J_1 M_1}^{(3)} \rho_{J_1 M_1 | J' M'}(t) - V_{J_1 M_1 | J' M'}^{(3)} \rho_{JM|J_1 M_1}(t) \\ & + 3\beta_{\perp} [V_{JM|J_1 M_1}^{(1)} \rho_{J_1 M_1 | J' M'}(t) - V_{J_1 M_1 | J' M'}^{(1)} \rho_{JM|J_1 M_1}(t)]\}, \end{aligned} \quad (12)$$

with  $V_{JM|J'M'}^{(i)} = \langle JM | \cos^i \theta | J'M' \rangle$  ( $i = 1, 2, 3$ ) and  $\epsilon_J = B_e J(J+1)$ . We can solve the above equation by using the

fourth-order Runge-Kutta method with the initial density operator following the temperature-dependent Boltzmann distribution,

$$\rho_0(T) = \frac{1}{Z} \sum_{J=0}^{\infty} \sum_{M=-J}^{M=J} |JM\rangle \langle JM| \exp\left[\frac{-B_e J(J+1)}{K_B T}\right], \quad (13)$$

where

$$Z = \sum_{J=0}^{\infty} \sum_{M=-J}^{M=J} \exp\left[\frac{-B_e J(J+1)}{K_B T}\right] \quad (14)$$

is the partition function with the Boltzmann constant  $K_B$  at the temperature  $T$ .

### 3. Results and Discussion

In this work, the parameters of the linear polarization molecule CO are as follows:  $B_e = 1.93 \text{ cm}^{-1}$ ,  $\mu = 0.112D$ ,  $\alpha_{\parallel} = 2.294 \text{ \AA}^3$ ,  $\alpha_{\perp} = 1.77 \text{ \AA}^3$ ,  $\beta_{\parallel} = 2.748 \times 10^9 \text{ \AA}^5$ , and  $\beta_{\perp} = 4.994 \times 10^8 \text{ \AA}^5$ . The two-color laser pulse combined with THz laser pulse is used to modulate the collision-induced orientation. The two-color field parameters are set to  $\sigma_r = 20 \text{ ps}$ ,  $\sigma_f = 0.4 \text{ ps}$ ,  $E_{01} = 5.1 \times 10^7 \text{ V/cm}$ , and  $\omega_1 = 12,500 \text{ cm}^{-1}$ . The THz laser pulse parameters are  $E_{02} = 1.0 \times 10^7 \text{ V/cm}$ ,  $t_d = 2.16 \text{ ps}$ ,  $\tau = 450 \text{ ps}$ ,  $\varphi = \pi$ , and  $\omega_{\text{THz}} = 36 \text{ cm}^{-1}$ . Since at approximately zero thermal energy, the molecule is generally in low and stable rotational states, for convenience to investigate, the temperature  $T = 0 \text{ K}$  is selected initially.

For clearly exhibiting the effect of the external fields on the collision-induced orientation, we first explore the time evolution of the molecular orientation under different conditions in Fig. 2. Figure 2(a) presents the orientation in the absence of an external field, and Fig. 2(b) shows the orientation degree in the THz field, the two-color field, and a combination of two laser pulses, respectively, where  $b = 6 \text{ a.u.}$ ,  $\nu = 0.03 \text{ a.u.}$ , and a.u. is atomic unit throughout the text. We can see that the orientation takes on the reciprocating oscillation around  $t = nT_{\text{rot}}$  ( $n = 0, 1, 2, \dots, n$ ) in all cases, with the rotational period of the molecule  $T_{\text{rot}} = 8.64 \text{ ps}$ . In the absence of an external field, the maximum of orientation is only 0.0017 in Fig. 2(a). However, in the presence of external fields, the maximum of orientation corresponding to three different pulses is 0.2896, 0.7799, and 0.7930 in Fig. 2(b), respectively. Obviously, compared with the absence of an external field, the orientation is largely improved when laser pulses are added, and, relative to the single pulse condition, the combination fields achieve a better degree of orientation. The result shows that the collision-induced orientation can be improved to some extent under the combined field.

To display the variation of the maximal degree of orientation  $\langle \cos \theta \rangle_{\text{max}}$  with the collision velocity and impact parameter under the combined field modulation, we depict the curves of  $\langle \cos \theta \rangle_{\text{max}}(v, b)$  in Fig. 3. Here, the velocities are 0.03, 0.05, 0.07, and 0.09 a.u., and the impact parameters are 6, 8, 10,

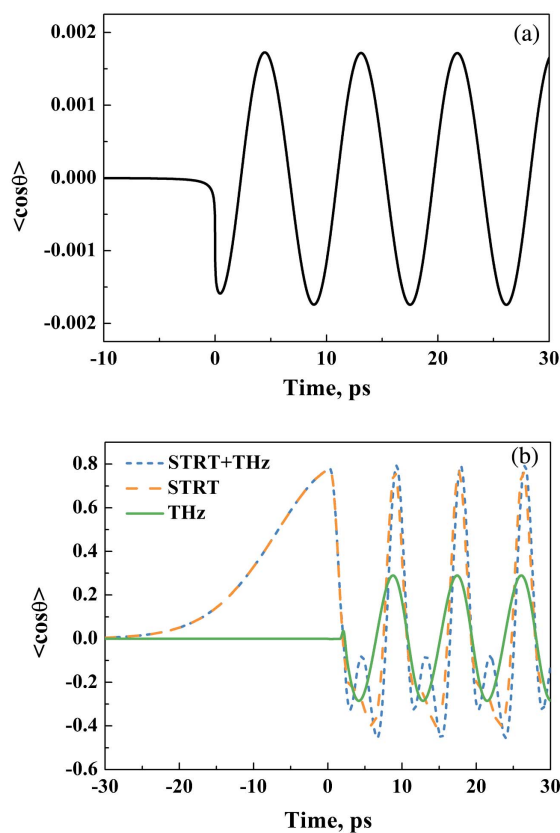


**Fig. 2.** Time evolution of the molecular orientation (a) in the absence of an external field and (b) being steered by laser pulses. Green line, THz laser pulse; orange line, two-color laser pulse; blue line, combination of two laser pulses.  $b = 10$  a.u.,  $v = 0.06$  a.u.,  $E_{01} = 5.1 \times 10^7$  V/cm,  $E_{02} = 1.0 \times 10^7$  V/cm,  $\tau = 450$  ps,  $\omega_1 = 12,500$   $\text{cm}^{-1}$ ,  $t_d = 2.16$  ps,  $\omega_{\text{THz}} = 36$   $\text{cm}^{-1}$ ,  $\varphi = \pi$ , and  $T = 0$  K in all.

and 12 a.u. It can be seen from Fig. 3(a) that with the increase of the collision velocity, the maximal degree of orientation  $\langle \cos \theta \rangle_{\text{max}}$  decreases gradually and becomes stable in the end. The reason for this can be that the increase of the collision energy will lead to the decrease of the collision cross section. Meanwhile, in the same collisional velocity, the  $\langle \cos \theta \rangle_{\text{max}}$  is decreasing with the increasing of impact parameter in Fig. 3(b), which is because the increase of the impact parameter means the increase of the collision distance between  $\text{H}^+$  and the CO molecule; as a result, the interaction force between them is decreasing gradually. From the above discussion, we can conclude that the collision-induced maximal orientation degree under the combined fields gradually decreases with the collisional velocity and impact parameter increasing. Although both of the parameters can change the molecular orientation, the influences are still too small to be actually used. Obviously, changing the molecular orientation substantially must resort to the external field factors.

To this end, we explore the impact of optimized two-color and THz field intensity on the molecular orientation induced by the  $\text{H}^+$  collision. The maximal degree of orientation versus the laser amplitude is given in Fig. 4, where the impact parameter is 5 a.u.,

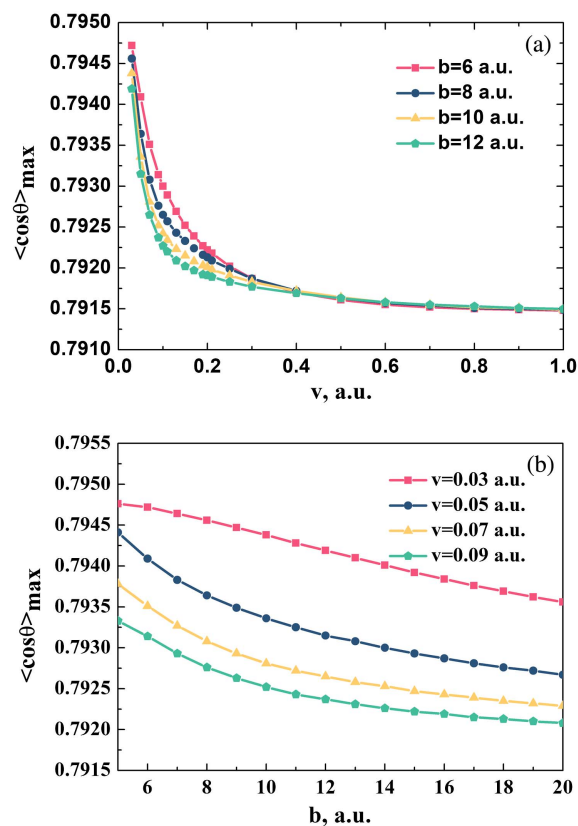


**Fig. 3.** Maximal degree of orientation as a function of the (a) collision velocity and (b) impact parameter.

and the velocity is 0.03 a.u. Figure 4(a) shows that the maximal degree of orientation  $\langle \cos \theta \rangle_{\text{max}}$  increases from 0.305 to 0.798 when the two-color field intensity varies from  $3.0 \times 10^7$  to  $5.2 \times 10^7$  V/cm; later it decreases gradually as the two-color field intensity varies from  $5.2 \times 10^7$  to  $7.0 \times 10^7$  V/cm, where  $E_{02} = 1.0 \times 10^7$  V/cm. The reason is that the orientation is not an adiabatic process for this situation, so the degree of orientation increases at first and later decreases with increasing two-color field intensity. With regard to the THz field intensity in Fig. 4(b), the amplitude varies from  $0.05 \times 10^7$  to  $1.5 \times 10^7$  V/cm, where  $E_{01} = 5.2 \times 10^7$  V/cm. The maximal orientation degree increases from 0.8015 to 0.8117 when THz field intensity varies from  $0.05 \times 10^7$  to  $0.45 \times 10^7$  V/cm, and next it decreases gradually from 0.8117 to 0.7744 when the THz field amplitude changes from  $0.45 \times 10^7$  to  $1.5 \times 10^7$  V/cm. This trend is due to the shift of rotational energy level with the increase of THz field intensity. As can be seen from the above results, selecting the appropriate two-color and THz laser pulse intensity is beneficial to improving the molecular orientation.

The CEP and frequency are significant parameters of THz laser pulse. Figure 5 shows the maximal degree of molecular orientation as a function of the CEP and frequency. As we can see from Fig. 5(a), by changing the THz laser pulse CEP from 0 to  $4\pi$ , the maximal degree of orientation first increases and

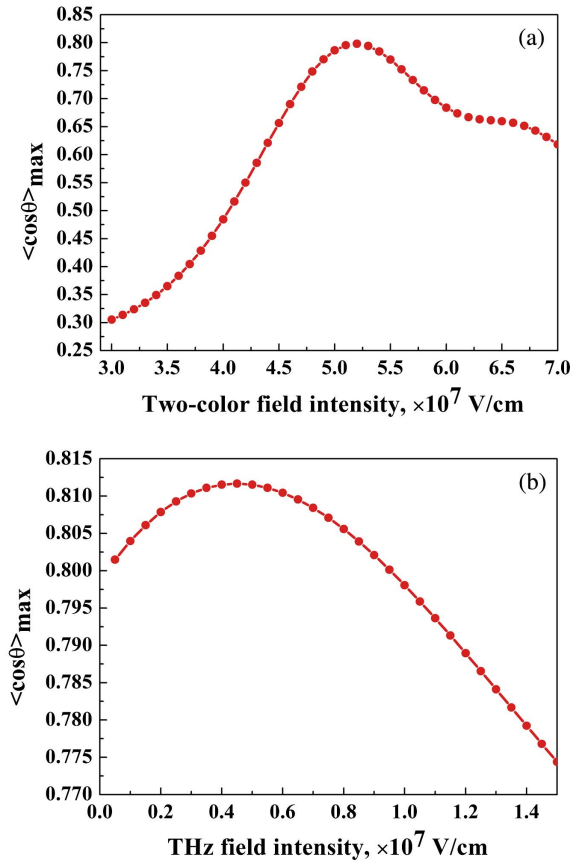


Fig. 4. Maximal degree of orientation  $\langle \cos \theta \rangle_{\max}$  as a function of the field intensity of the (a) two-color and (b) THz field, where the  $b = 5$  a.u.,  $v = 0.03$  a.u., and  $T = 0$  K.

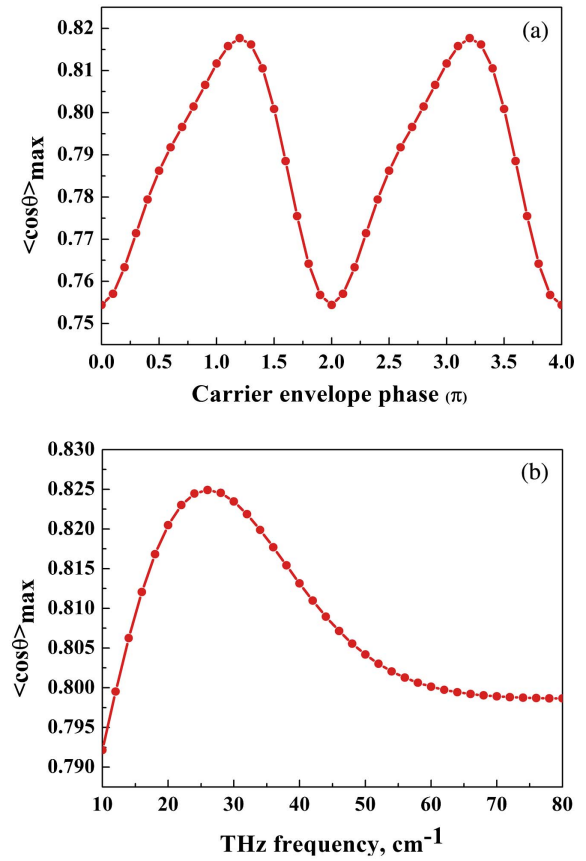
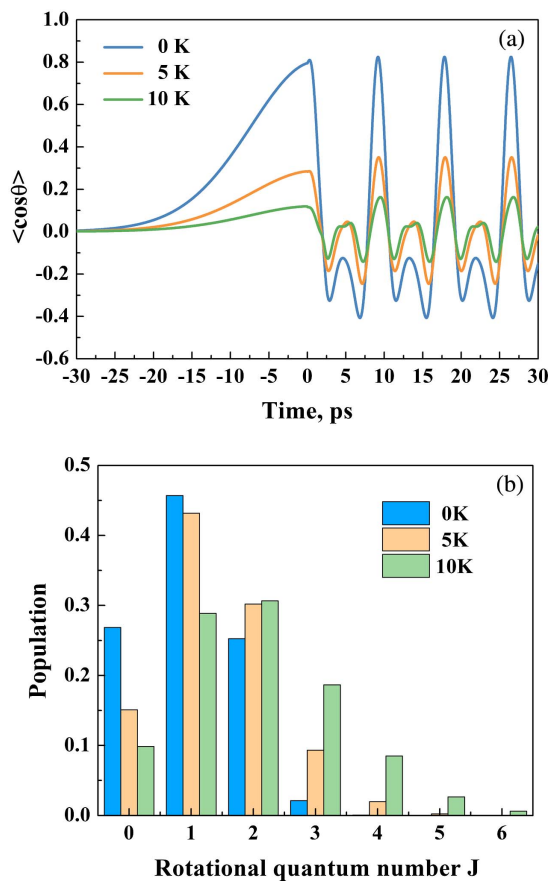


Fig. 5. Maximal degree of the orientation  $\langle \cos \theta \rangle_{\max}$  as a function of the (a) CEP and (b) frequency of the THz laser pulse, where  $b = 5$  a.u.,  $v = 0.03$  a.u.,  $E_{01} = 5.2 \times 10^7$  V/cm,  $E_{021} = 0.45 \times 10^7$  V/cm, and  $T = 0$  K.

then decreases in a period of  $2\pi$ . By regulating the CEP, the obtained changing range of the maximal orientation degree is between 0.7544 and 0.8177, corresponding to a CEP range between  $\varphi = 0\pi$  and  $1.2\pi$ . From this result, it can be found that the change amplitude of the maximal orientation is only 0.0633. Compared with the change obtained without the collision induction by Liu *et al.*<sup>[36]</sup>, this value is relatively small, but the initial maximal orientation degree is obviously improved. So, we can get that, in the case of combined pulses, although the CEP of THz laser pulses has little effect on the maximal degree of orientation change, it is undeniable that CEP is still an effective parameter to enhance the molecular maximum orientation degree. Figure 5(b) shows that when the THz frequency varies from 10 to  $80 \text{ cm}^{-1}$ , the maximal degree of orientation presents a trend of first increasing and then decreasing with the increase of THz frequency. As can be achieved from this figure, the maximal orientation degree increases from 0.792 to 0.825 ( $\Delta \cos \theta_{\max} = 0.033$ ) when the THz field frequency  $\omega_{\text{THz}}$  varies from 10 to  $26 \text{ cm}^{-1}$ . The maximum corresponds to the resonant interaction between the molecule and THz laser pulse. As the THz frequency continues to increase, the maximal molecular orientation degree gradually decreases and tends to be stable. In short, the selection of THz laser pulse CEP and

frequency parameter must be seriously considered for getting a maximal molecular orientation degree under the combined field.

What was discussed above mainly concentrates on the effect of pulse and interaction parameters at temperature of 0 K. To further explore the influence of temperature on orientation degree, we changed the system temperature to investigate the degree of orientation induced by collision and modulated with combined laser pulses. Figure 6(a) gives the time evolution curves of molecular orientation under different temperatures. We can acquire the maximal orientation degrees of 0.825, 0.351, and 0.163 when the temperature  $T = 0, 5,$  and 10 K in order. Clearly, the temperature affects the orientation degree greatly, and a higher orientation degree can be obtained at a lower temperature. To interpret the influence of temperature on the rotational population of molecules, we represent the population of different rotational states at three rotation temperatures in Fig. 6(b), where the selection of temperature is the same as in Fig. 6(a). Evidently, the rotational population transfers from at most three to at most four with the temperature increasing from 0 to 5 K, and, when the temperature goes up to 10 K, this population transfer is even more pronounced. This tendency coincides with the temperature-dependent



**Fig. 6.** (a) Time evolution curves of orientation degree and (b) the rotational population of different rotational states at the temperature  $T = 0$  K (blue line), 5 K (orange line), and 10 K (green line), while  $b = 5$  a.u.,  $v = 0.03$  a.u.,  $E_{01} = 5.2 \times 10^7$  V/cm,  $E_{02} = 0.45 \times 10^7$  V/cm,  $\varphi = 1.2\pi$ , and  $\omega_{\text{THz}} = 26$   $\text{cm}^{-1}$ .

Boltzmann distribution, i.e., more rotational states will be populated at non-zero temperature. Thus, the maximal molecular orientation degree will increase as the temperature decreases.

#### 4. Conclusion

In this work, the orientation of molecules induced by the  $\text{H}^+$  collision and modulated with combined fields has been studied theoretically. A better degree of orientation is obtained by the combination fields than by the absence of the external field or single laser pulse condition. It is found that the increase of collision velocity can lead to the decrease of the collision cross section and result in the decrease of the maximal orientation degree, while the increase of the collision parameter can give rise to the decrease of the interaction force between the ion and molecule, which is also the reason for decreasing the maximal degree of orientation. An improved orientation degree is achieved by adjusting the two-color laser pulse and THz field intensity, CEP, and THz frequency. From the time evolution of molecular orientation at different temperatures and the variation of rotational population of different rotational states, it can be seen that a higher orientation degree can be achieved at lower

temperatures. We hope that the theoretical result can be used as a reference for future experiments.

#### Acknowledgement

This work was supported by the National Natural Science Foundation of China (No. 11674198) and the Taishan Scholar Project of Shandong Province (No. ts201511025). We also thank Prof. Shulin Cong from Dalian University of Technology for providing the original FORTRAN code.

#### References

- L. Holmegaard, J. L. Hansen, L. Kalhøj, S. L. Kragh, H. Stapelfeldt, F. Filsinger, J. Kupper, G. Meijer, D. Dimitrovski, M. Abu-Samha, C. P. J. Martiny, and L. B. Madsen, "Photoelectron angular distributions from strong-field ionization of oriented molecules," *Nat. Phys.* **6**, 428 (2010).
- J. L. Hansen, H. Stapelfeldt, D. Dimitrovski, M. Abu-Samha, C. P. Martiny, and L. B. Madsen, "Time-resolved photoelectron angular distributions from strong-field ionization of rotating naphthalene molecules," *Phys. Rev. Lett.* **106**, 073001 (2011).
- J. Hu, M. S. Wang, K. L. Han, and G. Z. He, "Attosecond resolution quantum dynamics between electrons and  $\text{H}_2^+$  molecules," *Phys. Rev. A* **74**, 063417 (2006).
- J. Hu, K. L. Han, and G. Z. He, "Correlation quantum dynamics between an electron and  $\text{D}_2^+$  molecule with attosecond resolution," *Phys. Rev. Lett.* **95**, 123001 (2005).
- T. Kanai, S. Minemoto, and H. Sakai, "Quantum interference during high-order harmonic generation from aligned molecules," *Nature* **435**, 470 (2005).
- H. M. Wu, S. J. Yue, J. B. Li, S. L. Fu, B. Hu, and H. C. Du, "Controlling non-adiabatic spectral redshift of high-order harmonic using two orthogonally polarized laser fields," *Chin. Opt. Lett.* **16**, 040203 (2018).
- T. Kanai, S. Minemoto, and H. Sakai, "Ellipticity dependence of high-order harmonic generation from aligned molecules," *Phys. Rev. Lett.* **98**, 053002 (2007).
- D. Dimitrovski, J. Maurer, H. Stapelfeldt, and L. B. Madsen, "Observation of low-energy electrons in the photoelectron energy distribution from strong-field ionization of naphthalene by circularly polarized pulses," *J. Phys. B* **48**, 121001 (2015).
- R. Siemering, O. Njaya, T. Weinacht, and R. De. Vivie-Riedle, "Field-dressed orbitals in strong-field molecular ionization," *Phys. Rev. A* **92**, 042515 (2015).
- Z. Y. Zhao, Y. C. Han, J. Yu, and S. L. Cong, "The influence of field-free orientation on the predissociation dynamics of the NaI molecule," *J. Chem. Phys.* **140**, 044316 (2014).
- T. P. Rakitzis, A. J. van den Brom, and M. H. M. Janssen, "Directional dynamics in the photodissociation of oriented molecules," *Science* **303**, 1852 (2004).
- J. Z. Shao, X. Liang, L. B. You, N. Pang, Y. Lin, S. M. Wang, Z. H. Deng, X. D. Fang, and X. Wang, "Laser-induced damage and periodic stripe structures of a  $\text{CaF}_2$  single crystal by an ArF excimer laser," *Chin. Opt. Lett.* **18**, 021403 (2020).
- Q. Guo, T. Liu, X. Q. Wang, Z. G. Zheng, A. Kudreyko, H. J. Zhao, V. Chigrinov, and H. S. Kwok, "Ferroelectric liquid crystals for fast switchable circular Damman grating," *Chin. Opt. Lett.* **18**, 080002 (2020).
- L. B. Madsen, J. P. Hansen, and J. Kocbach, "Excitation in ion-atom collisions inside subfemtosecond laser pulses," *Phys. Rev. Lett.* **89**, 093202 (2002).
- V. Prasad and K. Yamashita, "Effect of laser field ellipticity on the rovibrational excitations of a diatomic molecule," *Chem. Phys. Lett.* **426**, 8 (2006).
- Z. Z. Lu, D. Y. Chen, R. W. Fan, and Y. Q. Xia, "Laser-induced quadrupole-quadrupole collisional energy transfer in Xe-Kr systems," *Phys. Rev. A* **85**, 063402 (2012).
- H. Y. Zhang, D. Y. Chen, Z. Z. Lu, R. W. Fan, and Y. Q. Xia, "Numerical calculation of laser-induced collisional energy transfer in Ba-Sr system," *Acta Phys. Sin.* **57**, 7600 (2008).

18. G. Paterson, A. Relf, M. L. Costen, K. G. McKendrick, M. H. Alexander, and P. J. Dagdigan, "Rotationally elastic and inelastic dynamics of NO( $X^2\Pi$ ,  $v=0$ ) in collisions with Ar," *J. Chem. Phys.* **135**, 234304 (2011).
19. M. Brouard, S. D. S. Gordon, A. Hackett Boyle, C. G. Heid, B. Nichols, V. Walpole, F. J. Aoiz, and S. Stolte, "Integral steric asymmetry in the inelastic scattering of NO( $X^2\Pi$ )," *J. Chem. Phys.* **146**, 014302 (2017).
20. R. D. Levine and R. B. Bernstein, *Molecular Reaction Dynamics and Chemical Reactivity* (Oxford University, 1987).
21. M. Mohan and V. Prasad, "Laser-assisted vibrational excitations during ion-molecule collisions," *J. Phys. B* **24**, L81 (1991).
22. M. C. van Beek, J. J. ter Meulen, and M. H. Alexander, "Rotationally inelastic collisions of OH( $X^2\Pi$ ) + Ar. I. State-to-state cross sections," *J. Chem. Phys.* **113**, 628 (2000).
23. M. Brouard, H. Chadwick, S. D. S. Gordon, B. Hornung, B. Nichols, F. J. Aoiz, and S. Stolte, "Rotational orientation effects in NO(X) + Ar inelastic collisions," *J. Phys. Chem. A* **119**, 12404 (2015).
24. D. Zanuttini, I. Blum, E. di Russo, L. Rigutti, F. Vurpillot, J. Douady, E. Jacquet, P.-M. Anglade, and B. Gervais, "Dissociation of GaN $^{2+}$  and AlN $^{2+}$  in APT: analysis of experimental measurements," *J. Chem. Phys.* **149**, 134311 (2018).
25. E. Di Russo, I. Blum, I. Rivalta, J. Houard, G. Da Costa, F. Vurpillot, D. Blavette, and L. Rigutti, "Detecting dissociation dynamics of phosphorus molecular ions by atom probe tomography," *J. Phys. Chem. A* **124**, 10977 (2020).
26. R. B. Bernstein, "Analysis of the experimental orientation dependence of the reaction CH $_3$ I + Rb $\rightarrow$ RbI + CH $_3$ ," *J. Chem. Phys.* **82**, 3656 (1985).
27. B. Friedrich and D. Herschbach, "Enhanced orientation of polar molecules by combined electrostatic and nonresonant induced dipole forces," *J. Chem. Phys.* **111**, 6157 (1999).
28. L. Cai, J. Marango, and B. Friedrich, "Time-dependent alignment and orientation of molecules in combined electrostatic and pulsed nonresonant laser fields," *Phys. Rev. Lett.* **86**, 775 (2001).
29. S. A. Zhang, C. H. Lu, T. Q. Jia, Z. G. Wang, and Z. R. Sun, "Field-free molecular orientation enhanced by two dual-color laser subpulses," *J. Chem. Phys.* **135**, 034301 (2011).
30. J. Wu and H. P. Zeng, "Field-free molecular orientation control by two ultrashort dual-color laser pulses," *Phys. Rev. A* **81**, 053401 (2010).
31. S. A. Zhang, J. H. Shi, H. Zhang, T. Q. Jia, Z. G. Wang, and Z. R. Sun, "Field-free molecular orientation by a multicolor laser field," *Phys. Rev. A* **83**, 023416 (2011).
32. C. C. Shu, K. J. Yuan, W. H. Hu, J. Yang, and S. L. Cong, "Controlling the orientation of polar molecules in a rovibrationally selective manner with an infrared laser pulse and a delayed half-cycle pulse," *Phys. Rev. A* **78**, 055401 (2008).
33. Q. Y. Cheng, J. S. Liu, X. C. Zhou, Y. Z. Song, and Q. T. Meng, "Field-free alignment dynamics of FCN molecule induced by a terahertz half-cycle pulse," *Europhys. Lett.* **125**, 33001 (2019).
34. M. Muramatsu, M. Hita, S. Minemoto, and H. Sakai, "Field-free molecular orientation by an intense nonresonant two-color laser field with a slow turn on and rapid turn off," *Phys. Rev. A* **79**, 011403 (2009).
35. J. S. Liu, Q. Y. Cheng, D. G. Yue, X. C. Zhou, and Q. T. Meng, "Dynamical analysis of the effect of elliptically polarized laser pulses on molecular alignment and orientation," *Chin. Opt. Lett.* **16**, 103201 (2018).
36. Y. Liu, J. Li, J. Yu, and S. L. Cong, "Field-free molecular orientation by two-color shaped laser pulse with time-delayed THz laser pulse," *Laser Phys. Lett.* **10**, 076001 (2013).
37. J. S. Liu, Q. Y. Cheng, D. G. Yue, X. C. Zhou, and Q. T. Meng, "Influence factor analysis of field-free molecular orientation," *Chin. Phys. B* **27**, 033301 (2018).